Shear Wave Elastography and Quantitative Ultrasound as Biomarkers to Characterize Deep Vein Thrombosis In Vivo

Guillaume Bosio, BSc, Nora Zenati, MD, François Destrempes, PhD, Boris Chayer, MEng, Gilles Pernod, MD, Guy Cloutier, Eng, PhD

Received June 28, 2021, from the Institute of Biomedical Engineering, University of Montreal, Montréal, Québec, Canada (G.B., G.C.); Laboratory of Biorheology and Medical Ultrasonics, University of Montreal Hospital Research Center (CRCHUM), Montréal, Québec, Canada (G.B., F.D., B.C., G.C.); UGA UFRM—Université Grenoble Alpes—UFR Médecine, Grenoble, France (N.Z., G.P.); Centre Hospitalier Universitaire de Grenoble, Grenoble, France (G.P.); F-CRIN INNOVTE Network, Saint Etienne, France (G.P.); and Department of Radiology, Radio-Oncology and Nuclear Medicine, University of Montreal, Montréal, Québec, Canada (G.C.). Manuscript accepted for publication October 11, 2021.

We are grateful to Guillaume Flé for reviewing sections of this manuscript. Partial funding for this project was obtained from the Investigation Network on Venous Thrombo-Embolism of the French Clinical Research Infrastructure Network.

All of the authors of this article have reported no disclosures.

Address correspondence to Guy Cloutier, Eng, PhD, Laboratory of Biorheology and Medical Ultrasonics, University of Montreal Hospital Research Center, 900 St-Denis, Montréal, QC H2X 0A9, Canada.

E-mail: guy.cloutier@umontreal.ca

Abbreviations

DVT, deep vein thrombosis; HKD, homodyned K-distribution; IQ, in-phase and quadrature; PE, pulmonary embolism; QUS, quantitative ultrasound; RF, radio frequency; ROI, region of interest; rt-PA, recombinant tissue plasminogen activator; SWE, shear wave elastography

doi:10.1002/jum.15863

Objective—Investigate shear wave elastography (SWE) and quantitative ultrasound (QUS) parameters in patients hospitalized for lower limb deep vein thrombosis (DVT).

Method—Sixteen patients with DVT were recruited and underwent SWE and radiofrequency data acquisitions for QUS on day 0, day 7, and day 30 after the beginning of symptoms, in both proximal and distal zones of the clot identified on B-mode scan. SWE and QUS features were computed to differentiate between thrombi at day 0, day 7, and day 30 following treatment with heparin or oral anticoagulant. The Young's modulus from SWE was computed, as well as QUS homodyned K-distribution (HKD) parameters reflecting blood clot structure. Median and interquartile range of SWE and QUS parameters within clot were taken as features.

Results—In the proximal zone of the clot, the HKD ratio of coherent-to-diffuse backscatter median showed a significant decrease from day 7 to day 30 ($P = .036$), while the HKD ratio of diffuse-to-total backscatter median presented a significant increase from day 7 to day 30 ($P = .0491$). In the distal zone of the clot, the HKD normalized intensity of the echo envelope median showed a significant increase from day 0 to day 30 ($P = .0062$). No SWE features showed statistically significant differences over time. Nonetheless, a trend of lower median of Young's modulus within clot for patients who developed a pulmonary embolism was observed.

Conclusion—QUS features may be relevant to characterize clot's evolution over time. Further analysis of their clinical interpretation and validation on a larger dataset would deserve to be studied.

Key Words—homodyned K-distribution; quantitative ultrasound imaging; shear wave elastography imaging; ultrasonography; venous thrombosis

Blood clot formation is a natural response to endothelial damage or a pathological consequence of a particular condition (eg, blood flow stagnation). A deep vein thrombosis (DVT) consists of the formation of a clot (or clots) in a vein located deep inside the body, mainly the legs. DVT is common to an extent of 1 per 1000 persons each year (in the United States)[1,2] and can evolve into pulmonary embolism (PE), which occurs when the clot, or a part of it, travels in the circulatory system and blocks a downstream blood vessel in the lungs. Both DVT and PE are severe diseases, and DVT complications leading to an PE can be fatal.

When a clot occurs and is brought to medical attention, it is typically treated by anticoagulant therapy to avoid further complications.[3,4] The aim of the treatment is to stop the clot's progression and let the body dissolve it, rather than aiming at directly dissolving the clot. However, the risk of recurrence can yield uncertainty in the treatment's duration.[5,6] Patients with DVT who develop a PE present clots that are less compact, more permeable, and more susceptible to lysis than is the case in the absence of PE.[7]

The age of blood clots has been used as a feature to characterize them. Ultrasound strain and shear wave elastography (SWE) was specifically proposed to assess blood clots' aging *in vitro* and in animal models.[8–12] It could be demonstrated that older clots are stiffer. Clinical studies have also reported the usefulness of strain elastography to differentiate acute from chronic thrombi.[13,14] The effect of treatment on blood clot elasticity has also been investigated. Sutton et al[15] demonstrated *in vitro* and in animals the impact of clots' aging on their resistance to lysis: the older a clot, the more resistant it was to breaking up using ultrasound-induced thrombolysis. Mercado-Shekhar et al[16] investigated the effect of blood clots' retractation on Young's moduli from SWE, and on the efficacy of recombinant tissue plasminogen activator (rt-PA) usage. Highly retractable clots had higher Young's moduli and were more resistant to lyse than mildly retracted clots.

Quantitative ultrasound (QUS) imaging has also been investigated in the context of blood clotting analysis.[17–21] Sigel et al[22] showed *in vitro* that loose fibrin clots backscatter less energy (ie, hypoechoic on B-mode) in comparison with red blood cell-rich clots or dense fibrin clots. Another study highlighted the increase in echogenicity during clotting due to fibrin fiber formation.[23] Some studies have looked at the statistical distribution of backscatter echoes, notably using Nakagami parameters.[24,25] Fang et al[24] showed *in vitro* that Nakagami parameters were linked to the weight loss ratio of thrombus following treatment with a thrombolytic agent. They also reported[25] *in vitro* that Nakagami parameters decreased during thrombus aging. Another general model for statistical analysis of backscatter echoes that has not yet been investigated in the context of blood clot imaging is the homodyned K-distribution (HKD),[26] which can characterize microstructural properties of tissues.[27,28]

The characterization of blood clot properties may provide information about their scalable profile over time, and their amenability to embolization. *In vivo* thrombus characterization could also be relevant in predicting mechanical and structural evolution during anticoagulant therapy. The effect of treatment on patients with DVT remains to be studied using elastography and QUS methods. The first objective of this study was to investigate the evolution of blood clots in patients newly diagnosed and hospitalized for acute DVT using SWE and HKD imaging. The second objective was to assess if patients experiencing a PE had measurable impacts on ultrasound features of imaged blood clots.

Methods

Patients' recruitment, acquisition of ultrasound images, and manual delineation of clots on one frame were performed at the Center Hospitalier Universitaire de Grenoble, while the team at the research center of the Center Hospitalier de l'Université de Montréal provided the manual segmentation software, performed data processing, statistical, and data analyses. The study protocol (Clinical Trial NCT02859532) and informed consent were approved by the ethical committee of Institutional review boards of both centers, and the National Agency for Medicines Safety and Health Products. All participants signed an informed consent.

Inclusion and Exclusion Criteria

Inclusion criteria for participating in the study were patients over 18 years old, with a proximal DVT inducing symptoms for less than 3 days, experiencing a PE or not, treated with heparin or oral anticoagulant, and affiliated to social welfare. Exclusion criteria were pregnant or breastfeeding patients, an expected lifespan of less than 1 month, a distal or asymptomatic DVT, previous pharmacomechanical thrombolysis, and individuals in exclusion period from another study or under administrative surveillance or guardianship. A total of 16 patients were recruited from February 2017 to January 2019.

Study Conduct

DVT was diagnosed according to standard practice, that is, clinical evaluation using Wells score, and imaging by compression ultrasound. After diagnosis,

patients were immediately treated with heparin or oral anticoagulant. The first ultrasound acquisitions were made after informed written consent, within 1 or 2 days following admission and diagnosis, which we refer to as day 0. Other ultrasound acquisitions were made on day 7 and day 30 visits. All data were anonymized and transfer between teams was performed via a secure drop box in anonymized form.

For each set of acquisitions, the head and base of the clot were identified by use of a B-mode image acquired with an Aixplorer scanner (Aixplorer Multiwave, Supersonic Imagine, Aix-en-Provence, France). Using the SWE mode, image acquisitions were performed in a rectangular area, called Q-box, comprising the clot confirmed by four different clinicians with 5 years of expertise each in vascular imaging. Ultrasound data were saved on a workstation.

Figure 1. A, Example of a shear wave elastography image of an 84-year old female with a DVT and no PE. The region in which the acquisition was performed (rectangular area, called Q-box, in elastography and B-mode images) was selected prior to manual segmentation. The range of Young's moduli is represented by a colorbar in kPa. The colorbar varied between 0 and 180 kPa. **B-left,** Previously selected Q-box (as pointed by the arrow) that was used to manually delineate the clot's contours by a clinician. **B-right,** Result of the manual segmentation. The elastography feature extraction was restricted to this region of interest.

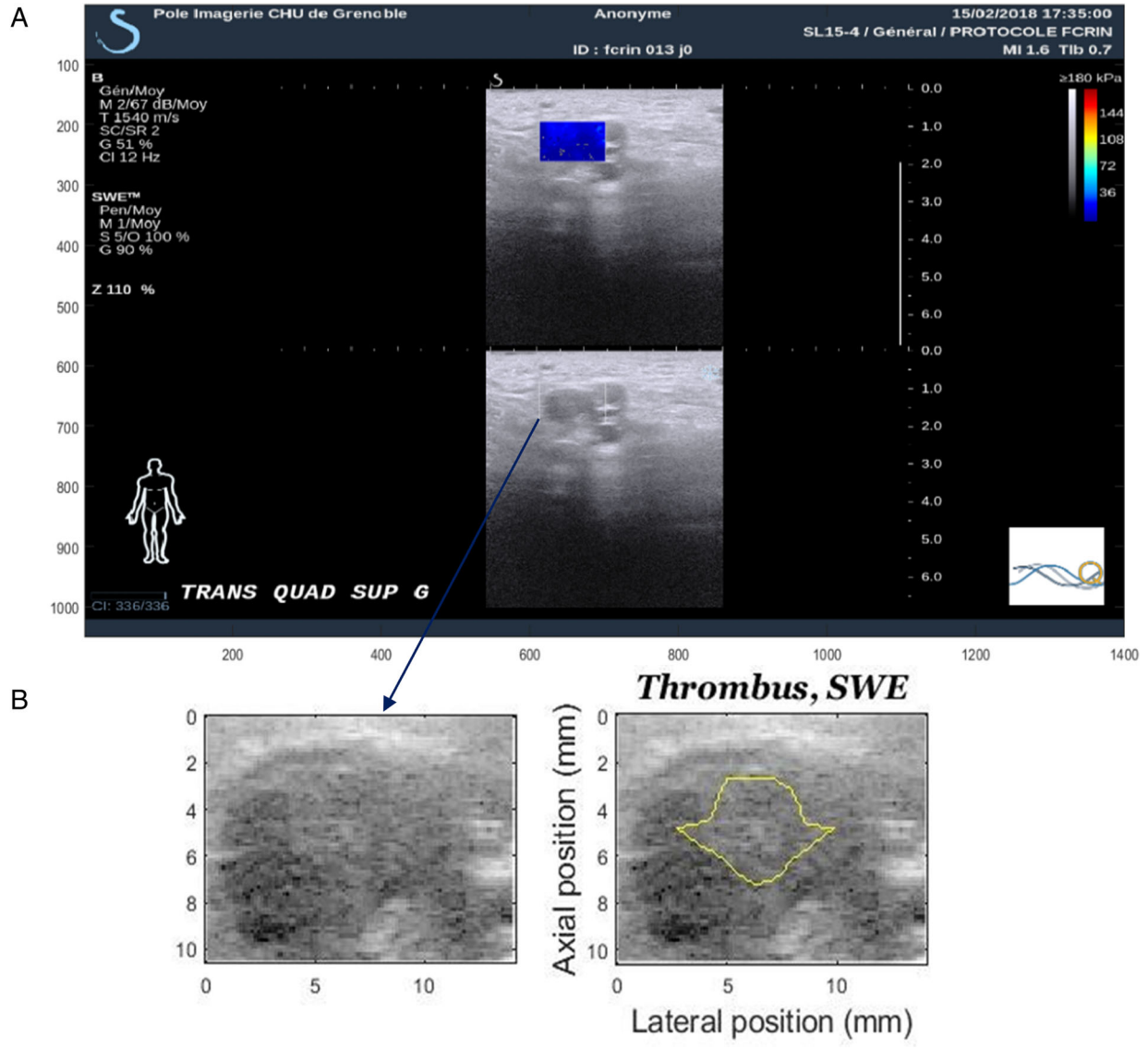

Two transversal-view acquisitions of four images each were acquired, one in the proximal zone of the thrombus and one in the distal zone. The distal measurement was located at the femoro-popliteal deep vein segment. The proximal one was performed at femoral or common femoral vein. Cineloops of in-phase and quadrature (IQ) raw data, which were converted to radio frequency (RF) data, comprising at least 50 frames, were also acquired in both proximal and distal zones using the research mode of the Aixplorer system.

Ultrasound data were formatted for the custom manual segmentation software, with prior manual delineation of a region of interest (ROI) within the clot identified by an ultrasound vascular thrombosis specialist. Example of a manual delineation can be found in Figure 1B. The ROI was delineated on one frame for each of the four sequences of images (proximal and distal zones, SWE, and RF data).

Post Processing

The first step of the post-processing was to propagate automatically, with a motion tracking algorithm, the ROI that was manually delineated on a frame on all remaining frames of each acquisition.[29] After this step, 4 or 50 images with segmented ROIs were available for each elastography or RF data acquisition, respectively.

The second step consisted of the extraction of SWE and statistical QUS features within segmented ROIs of each sequence of images. This step comprised calculation of the Young's modulus based on the recorded elasticity color maps, and calculation of HKD statistical parameters of the echo envelope of recorded RF data.[30]

Elastography Features

We report median and interquartile range (IQR) statistics of the Young's modulus E as elastography features. An example of an SWE image is provided in

Table 1. General Characteristics of the 16 Patients Included in the Study

Characteristics	Data
Sex	
Male	14 (87.5%)
Female	2 (12.5%)
Age (year)	
Mean ± SD (range)	73.5 ± 10.5 (49–88)
Pulmonary embolism (PE)	
Presence of PE	10 (62.5%)
Absence of PE	6 (37.5%)
Cancer	
Presence of cancer	4 (25%)
Absence of cancer	12 (75%)
Antiplatelet treatment	
Patient with antiplatelet treatment	3 (18.8%)
Patient without antiplatelet treatment	13 (81.2%)
Death	0
Beginning of symptoms before going to the hospital (days)	
DVT: mean ± SD (range)	3.4 ± 2.8 (0–8)
DVT with PE: mean ± SD (range)	4.3 ± 4.8 (1–15)
Treatment duration (months)	5.0 ± 1.4 (3–6)
Mean ± SD (range)	

SD, standard deviation.

Figure 2. An example of a parametric map with the corresponding B-mode image for parameter k (coherent-to-diffuse backscatter ratio). **Left,** A rectangular box (Q-box) within the B-mode image was selected by a clinician to better delineate the thrombus. **Right,** Value of k within the delineated ROI (in yellow). The patient is the same one as in Figure 1.

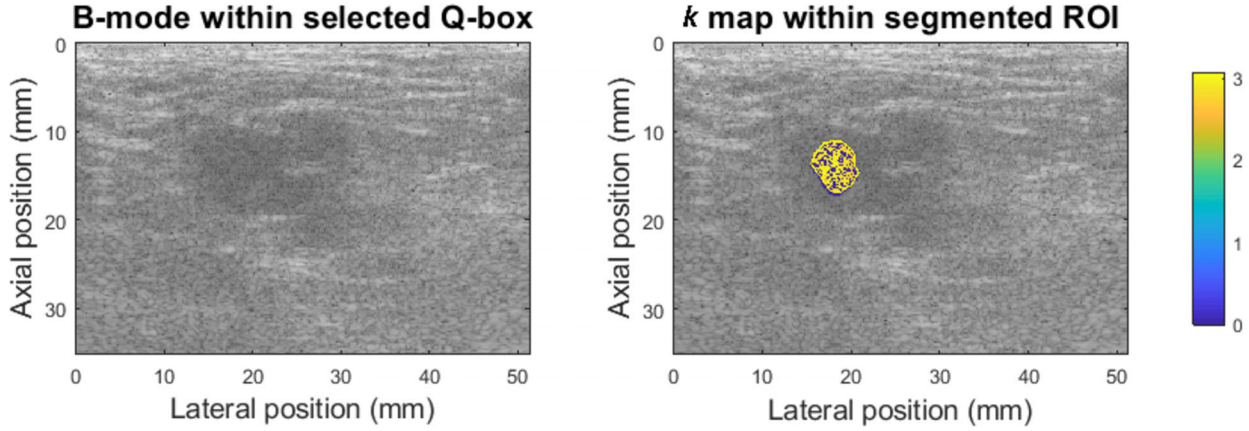

Figure 1A. The yellow ROI in Figure 1B was considered to compute the median and IQR of each feature that was evaluated over the four frames available.

Statistical QUS Features

We adopted the HKD statistical model of the echo envelope of RF data for QUS image analysis.[26,31] Four parameters of that model were considered: k, $1/(\kappa+1)$, μ_n, and $1/\alpha$. Parameter k is the ratio of coherent-to-diffuse backscatter signals; $1/(\kappa+1)$ represents the diffuse-to-total signal power ratio; μ_n is the normalized intensity of the echo envelope (mean value divided by the maximal value); and $1/\alpha$ is the reciprocal of the scatterer clustering parameter. Estimation of these parameters[32] within sliding windows of dimensions (4.5 mm axial [47 pixels] × 3 mm lateral [15 pixels]), with a 5% overlap rounded to the integer pixel yielded four HKD parametric maps.[30] For this purpose, pixels within the ROI were classified into three labels with a Monte Carlo algorithm based on echogenicity; for each window, only pixels with same label as the geometric center of the window were considered for the HKD estimation.[28] An example of a k map is displayed in Figure 2. On each map, median and IQR within the ROI were computed. The median value over the 50 frames of each feature was evaluated for blood clot analyses.

Statistical Analysis

Statistical analysis was performed with software R (version 3.6.3, R Foundation, Vienna, Austria). Shapiro–Wilk test was performed to assess the normality assumption of data. When the test was successful ($P > .1$), an analysis of variance test was performed to look for differences along time or

Table 2. Median and Interquartile Range Values of Young's Moduli With Presence or Absence of Pulmonary Embolism (PE) at Day 0

			Young's Moduli
			Mean ± SD (Over Patients)
Median (kPa)	Proximal	PE	6.0 ± 1.7
		No PE	6.7 ± 3.1
	Distal	PE	6.7 ± 1.2
		No PE	5.6 ± 0.7
Interquartile range (kPa)	Proximal	PE	2.1 ± 1.2
		No PE	3.2 ± 2.6
	Distal	PE	2.5 ± 1.6
		No PE	2.1 ± 0.7

No significant differences were observed between PE and no PE at any side (proximal or distal).
SD, standard deviation.

Figure 3. Median and IQR values of Young's moduli over segmented ROIs within clots. Different times are presented with different colors. *N* represents the number of patients for which acquisitions were available. No significant differences with Kruskal-Wallis test: $P > .05$.

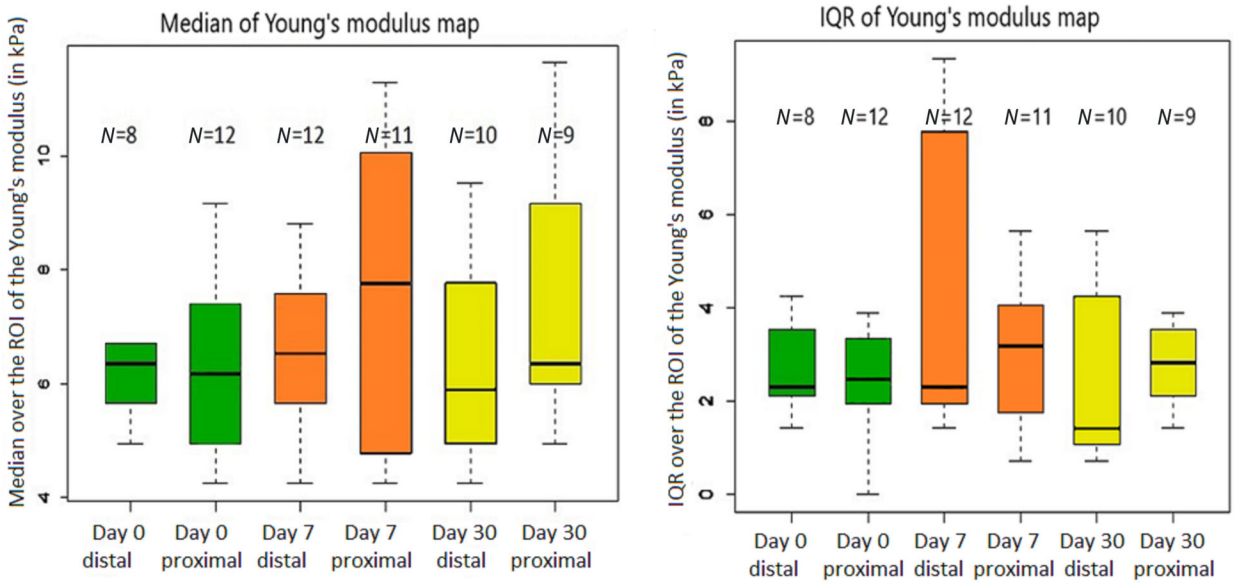

along the side (proximal or distal). In case of success ($P < .05$), post-hoc multiple pairwise comparisons were performed, applying the Holm-Bonferroni correction for *P*-values. When data were not normally distributed, the Kruskal-Wallis test was performed, followed by multiple pairwise comparisons

Figure 4. Median values of HKD parameters k, $1/(\kappa + 1)$, μ_n, and $1/\alpha$ over segmented ROIs within clots. Different times are presented with different colors. *N* represents the number of patients for which acquisitions were available. Parameters $1/(\kappa + 1)$, μ_n and $1/\alpha$ median have been tested with Kruskal-Wallis test followed (for $1/(\kappa + 1)$, μ_n) by a post-hoc multiple pairwise comparison (Wilcoxon) using the Holm-Bonferroni adjustment. ANOVA test followed by a post-hoc multiple pairwise comparison (*t*-test) using the Holm-Bonferroni adjustment has been performed on μ_n median. $^*P < .05$.

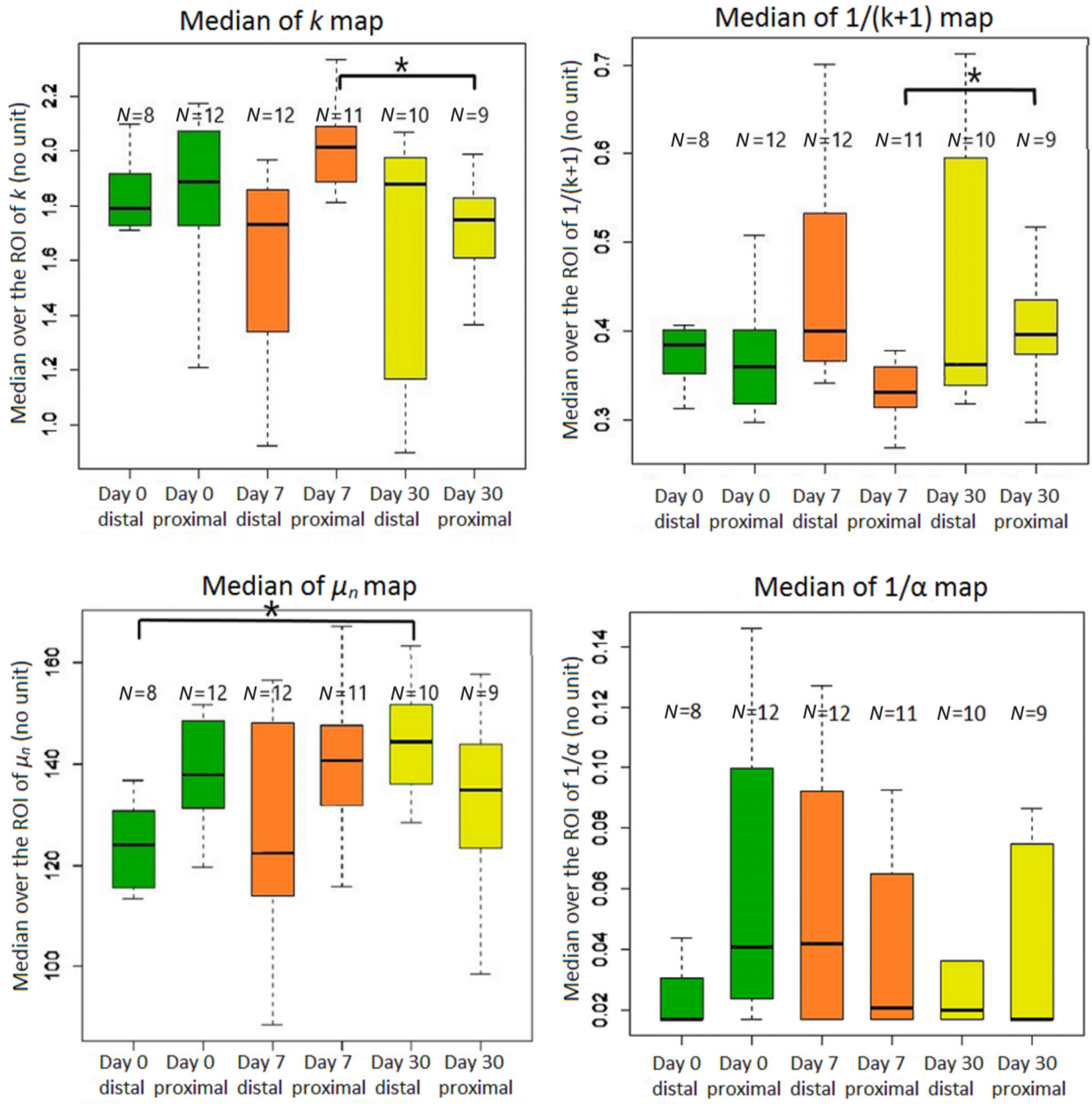

using the Holm-Bonferroni adjustment, in case of success ($P < .05$).

Results

Demographic and clinical information about the cohort can be seen in Table 1. Not all patients had data acquired at each day and on each leg side due to nonavailability of ultrasound systems or nonavailability of patients for a specific visit.

SWE Features

Figure 3 presents box plots of median and IQR values of Young's moduli E over time for proximal and distal measurements. A trend with median elasticity increasing from day 0 to day 7 then decreasing at day 30 can be observed, but there were no significant differences. No statistically significant differences were also found between proximal and distal parts of the thrombus at the various days.

The median and IQR of Young's moduli of deep vein thrombi were also compared between patients experiencing or not having a PE. We restricted the data analysis to day 0 to reduce the confounding effect of treatment. The aim was to see whether a day 0 thrombus, which would evolve into a PE, could be differentiated from a day 0 thrombus without PE evolution. There were 10 of the 16 patients who presented a PE. For day 0 data in the proximal view, there were acquisitions from 12 patients, 9 of which presented a PE. There were eight patients with distal acquisitions with five of them presenting a PE. Nonsignificant differences were found between groups of DVT that had evolved as a PE versus remaining ones. Mean values of SWE median and IQR for patients who developed a PE, and those who did not can be found in Table 2.

HKD Features

Figure 4 summarizes box plots for the median value of k, $1/(\kappa + 1)$, $\mu_{n,}$ and $1/\alpha$ within segmented ROIs. There was a significant decrease of k ($P = .036$) between day 7 and day 30 for the proximal segment, and a global significant difference ($P = .0395$) between distal and proximal measurements. For the median of $1/(\kappa + 1)$, a significant increase can be observed between day 7 and day 30 for the proximal segment ($P = .0491$). The median of HKD parameter μ_n presented also a significant difference ($P = .0062$) between day 0 and day 30, for distal measurements. Parameter $1/\alpha$ had no significant differences between time points and vessel segments. None of the four IQR parameters presented either any significant differences between time points and vessel segments (results not shown).

Similarly to SWE analyses, HKD parameters have been compared at day 0 to distinguish a thrombus evolving in a PE from a thrombus, which did not. Mean of HKD parameters of each group (PE vs. no PE) at day 0 for proximal and distal measurements can be found in Table 3. No significant differences were found.

Discussion

Clot evolution still raises a lot of questions and attention on how to better adapt the treatment, reduce hemorrhage risk due to treatment, understand which

Table 3. Median and Interquartile Range Values of Homodyned K-Distribution Parameters With Presence or Absence of Pulmonary Embolism (PE) at Day 0

			Mean ± SD (Over Patients)			
			k	$1/(\kappa + 1)$	μ_n	$1/\alpha$
Median (no unit)	Proximal	PE	1.84 ± 0.33	0.38 ± 0.10	144 ± 21	0.09 ± 0.11
		No PE	1.89 ± 0.22	0.36 ± 0.05	141 ± 6	0.06 ± 0.07
	Distal	PE	1.88 ± 0.16	0.36 ± 0.04	115 ± 27	0.02 ± 0.01
		No PE	1.19 ± 1.03	0.60 ± 0.36	123 ± 12	0.08 ± 0.11
Interquartile range (no unit)	Proximal	PE	1.05 ± 0.54	0.48 ± 0.59	226 ± 33	0.18 ± 0.07
		No PE	1.11 ± 0.36	0.26 ± 0.04	229 ± 18	0.20 ± 0.02
	Distal	PE	1.27 ± 0.46	0.68 ± 0.87	202 ± 34	0.23 ± 0.04
		No PE	0.73 ± 0.80	0.11 ± 0.13	201 ± 24	0.15 ± 0.11

No significant differences were observed between PE and no PE for any side or parameters.
SD, standard deviation.

clots would embolize, or find alternative treatments. To our knowledge, this study is the first of its kind to explore mechanical and QUS features over time on *in vivo* DVT data with administered anticoagulant drugs to patients.

No significant changes in Young's modulus features were observed in this study. Drugs administered to patients were heparin (for 1 or 2 days) or factor Xa inhibitor. Factor Xa acts at the end of the coagulation cascade by cleaving prothrombin into thrombin. Thrombin then converts soluble fibrinogen into insoluble fibrin strands. With inhibition of factor Xa, production of fibrin strands is stopped, thus preventing further evolution of the clot.[33] In a recent *ex vivo* study,[34] the Young's modulus of clots with different biological compositions and the effect of rt-PA on clot elasticity were investigated. In line with our results, they did not find any significant differences in clot's Young's modulus. In opposite, using mechanical testing on *in vitro* blood clot samples, fibrinolysis triggered by rt-PA reduced clot stiffness.[35] In our study, we expected changes in SWE parameters between day 0 and day 30 due to treatment and evolution of the clot. Our results were also expected to be different from other studies[9–11,14,16] because anticoagulant drugs were not used during the assessment of Young's moduli in these latter reports. Studies have shown that the density of clots is linked to the fibrin concentration.[36,37] Mercado-Shekhar et al[16] showed that high-density thrombi are linked to higher Young's moduli. By stopping fibrin production, the anticoagulant used could be responsible for the observed stagnation over time of blood clots' Young's modulus. Treatments lasted several months, and all clots were still present after 30 days. Changes in SWE measurements could have been observed if a longer period of observation had been considered until clots became close to final lysis.

Concerning PE, our hypothesis was that clots that end up embolizing are those with low values of Young's moduli (indicating softer blood clots). As results in Table 2 were not conclusive, a larger sample size would likely be required to validate or not this postulate.

The observed decrease in the median of k and increase in the median of $1/(\kappa + 1)$ within the proximal zone of clots after day 7 suggest a spatial disorganization of scatterers within the clot, as observed for other tissues.[29,38] An organized arrangement of scatterers could recall nearly periodic alignment of scatterers, or highly structured spatial organization of scatterers. A disorganized medium would have, on the contrary, close to uniformly positioned scatterers. A less organized medium, as suggested by parameters k and $1/(\kappa + 1)$, could indicate a risk of clot embolization into downstream pulmonary vessels, as was hypothesized in.[39]

The increase in the median of μ_n within distal measurement of clots between day 0 and day 30 corresponds to an increase in the normalized intensity of the echo envelope. These results indicate that despite the effect of oral anticoagulant, a clot is not getting dissolved yet and probably still contains fibrin strands or red blood cells, which are known to be echogenic.[22] Animal experiments with treated clots and histological analysis may allow testing this hypothesis.

In conclusion, measuring *in vivo* biomarkers without resorting at invasive procedure is still a challenge in medical practice. Concerning blood clots, an ultrasound marker of their evolution could be relevant to adapt the treatment's dose or duration.

Study Limitations

In this study, data from 16 patients were analyzed. In addition, few patients' data were available at day 0, and three patients had full data available (distal and proximal at all days), which reduced the power of statistical tests. Thus, the small number of recruited patients is a limitation of this study. The nonavailability at given time points of the ultrasound scanner or technicians is also a limitation. Because the intake of blood thinners and their effect on blood clot's Young's modulus or HKD parameters has not been reported, it is difficult to reach strong conclusions when it comes to their effect. The study could have benefited from a marker, such as the size of clot, to confirm the effect of the treatment but such measurements on B-mode images might not be conclusive due to variable echogenicity. Another limitation lies in the lack of deeper biological interpretation of QUS parameters in the characterization of blood clots. Future work could focus on the interpretation of HKD biomarkers based on histological analysis, but this would be difficult in the context of this *in vivo* 30-days follow-up study. A larger study cohort could allow testing whether Young's modulus or

HKD parameters may be used as predictors of pulmonary embolization. Assessing quantitatively on *in vitro* data the effect of treatment on blood clots based on Young's modulus or HKD parameters could also be relevant.

References

1. White RH. The epidemiology of venous thromboembolism. *Circulation* 2003; 107:I–4.
2. Heit JA. Epidemiology of venous thromboembolism. *Nat Rev Cardiol* 2015; 12:464–474.
3. Scarvelis D, Wells PS. Diagnosis and treatment of deep-vein thrombosis. *CMAJ* 2006; 175:1087–1092.
4. Wells P, Anderson D. The diagnosis and treatment of venous thromboembolism. *Hematology Am Soc Hematol Educ Program* 2013; 2013:457–463.
5. Baglin T, Luddington R, Brown K, Baglin C. Incidence of recurrent venous thromboembolism in relation to clinical and thrombophilic risk factors: prospective cohort study. *Lancet* 2003; 362:523–526.
6. Rodger MA, Kahn SR, Wells PS, et al. Identifying unprovoked thromboembolism patients at low risk for recurrence who can discontinue anticoagulant therapy. *CMAJ* 2008; 179:417–426.
7. Kupis RW, Goldman-mazur S, Polak M, Ząbczyk M, Undas A. Faster fibrin clot degradation characterizes patients with central pulmonary embolism at a low risk of recurrent peripheral embolism. *Sci Rep* 2019; 9:1–8.
8. Emelianov SY, Chen X, O'Donnell M, et al. Triplex ultrasound: elasticity imaging to age deep venous thrombosis. *Ultrasound Med Biol* 2002; 28:757–767.
9. Gennisson JL, Lerouge S, Cloutier G. Assessment by transient elastography of the viscoelastic properties of blood during clotting. *Ultrasound Med Biol* 2006; 32:1529–1537.
10. Schmitt C, Hadj Henni A, Cloutier G. Characterization of blood clot viscoelasticity by dynamic ultrasound elastography and modeling of the rheological behavior. *J Biomech* 2011; 44:622–629.
11. Mfoumou E, Tripette J, Blostein M, Cloutier G. Time-dependent hardening of blood clots quantitatively measured in vivo with shear-wave ultrasound imaging in a rabbit model of venous thrombosis. *Thromb Res* 2014; 133:265–271.
12. Liu X, Li N, Wen C. Effect of pathological heterogeneity on shear wave elasticity imaging in the staging of deep venous thrombosis. *PLoS One* 2017; 12:1–15.
13. Rubin JM, Xie H, Kim K, et al. Sonographic elasticity imaging of acute and chronic deep venous thrombosis in humans. *J Ultrasound Med* 2006; 25:1179–1186.
14. Yi X, Wei X, Wang Y, et al. Role of real-time elastography in assessing the stage of thrombus. *Int Angiol* 2017; 36:59–63.
15. Sutton JT, Ivancevich NM, Perrin SR, Vela DC, Holland CK. Clot retraction affects the extent of ultrasound-enhanced thrombolysis in an ex vivo porcine thrombosis model. *Ultrasound Med Biol* 2013; 39:813–824.
16. Mercado-Shekhar KP, Kleven RT, Aponte Rivera H, et al. Effect of clot stiffness on recombinant tissue plasminogen activator lytic susceptibility in vitro. *Ultrasound Med Biol* 2018; 44:2710–2727.
17. Jacobs JE, Malinka AV, Haque P, Jhabvala MD. Ultrasound spectroscopy applied to blood coagulation studies. *Ultrasonics* 1976; 14: 84–90.
18. Voleišis A, Kažys R, Mažeika L, et al. Ultrasonic method for the whole blood coagulation analysis. *Ultrasonics* 2002; 40:101–107.
19. Voleisis A, Kazys R, Voleisiene B, Sliteris R, Mazeika L. Ultrasonic method for monitoring the clotting process during whole blood coagulation. *Ultrasonics* 2017; 78:146–151.
20. Calor-Filho MM, Machado JC. Measurement of the ultrasonic attenuation coefficient of human blood plasma during clotting in the frequency range of 8 to 22 MHz. *Ultrasound Med Biol* 2006; 32:1055–1064.
21. Shung KP, Sigelmann RA, Schmer G. Ultrasonic measurement of blood coagulation time. *IEEE Trans Biomed Eng* 1975; 22: 334–337.
22. Sigel B, Feleppa EJ, Swami V, et al. Ultrasonic tissue characterization of blood clots. *Surg Clin North Am* 1990; 70:13–29.
23. Huang CC, Wang SH, Tsui PH. Detection of blood coagulation and clot formation using quantitative ultrasonic parameters. *Ultrasound Med Biol* 2005; 31:1567–1573.
24. Fang J, Tsui PH. Evaluation of thrombolysis by using ultrasonic imaging: an in vitro study. *Sci Rep* 2015; 5:1–12.
25. Fang J, Chen CK, Peng JY, et al. Changes in backscattered ultrasonic envelope statistics as a function of thrombus age: an in vitro study. *Ultrasound Med Biol* 2015; 41:498–508.
26. Dutt V, Greenleaf JF. Ultrasound echo envelope analysis using a homodyned K distribution signal model. *Ultrasonic Imaging* 1994; 16:265–287.
27. Trop I, Destrempes F, El Khoury M, et al. The added value of statistical modeling of backscatter properties in the management of breast lesions at US. *Radiology* 2015; 275:666–674.
28. Destrempes F, Franceschini E, Yu FTH, Cloutier G. Unifying concepts of statistical and spectral quantitative ultrasound techniques. *IEEE Trans Med Imaging* 2016; 35:488–500.
29. Destrempes F, Meunier J, Giroux MF, Soulez G, Cloutier G. Segmentation of plaques in sequences of ultrasonic B-mode images of carotid arteries based on motion estimation and a bayesian model. *IEEE Trans Biomed Eng* 2011; 58:2202–2211.
30. Roy-Cardinal MH, Destrempes F, Soulez G, Cloutier G. Assessment of carotid artery plaque components with machine learning classification using homodyned-K parametric maps and elastograms. *IEEE Trans Ultrason Ferroelectr Freq Control* 2019; 66:493–504.

31. Destrempes F, Cloutier G. A critical review and uniformized representation of statistical distributions modeling the ultrasound echo envelope. *Ultrasound Med Biol* 2010; 36:1037–1051.
32. Destrempes F, Porée J, Cloutier G. Estimation method of the homodyned K-distribution based on the mean intensity and two log-moments. *SIAM J Imaging Sci* 2013; 6:1499–1530.
33. Christos S, Naples R. Anticoagulation reversal and treatment strategies in major bleeding: update 2016. *West J Emerg Med* 2016; 17:264–270.
34. Hendley SA, Dimov A, Bhargava A, et al. Composition and thrombolytic susceptibility of ex vivo venous thromboembolism. *Sci Rep* 2021; https://www.researchsquare.com/article/rs-739402/v1. Accessed date September 2021.
35. Dwivedi A, Glynn A, Johnson S, et al. Measuring the effect of thrombosis, thrombus maturation and thrombolysis on clot mechanical properties in an in-vitro model. *J Biomech* 2021; 129:1107311–1107318.
36. Shah GA, Nair CH, Dhall DP. Physiological studies on fibrin network structure. *Thromb Res* 1985; 40:181–188.
37. Ryan EA, Mockros LF, Weisel JW, Lorand L. Structural origins of fibrin clot rheology. *Biophys J* 1999; 77:2813–2826.
38. Hruska DP, Oelze ML. Improved parameter estimates based on the homodyned K distribution. *IEEE Trans Ultrason Ferroelectr Freq Control* 2009; 56:2471–2481.
39. Kolecki RV, Sigel B, Justin J, et al. Determining the acuteness and stability of deep venous thrombosis by ultrasonic tissue characterization. *J Vasc Surg* 1995; 21:976–984.